The relaxation times were calculated using the standard "inversion–recovery" method while autostacking the data. These data were analyzed by using the commercial data tabulation program supplied by JEOL.

Acknowledgment. I thank the Monsanto Industrial Chemicals Applied Science Research and Development Group for making available the use of their JEOL FX-90Q heteronuclear NMR spectrometer, specifically B. Katlafsky and E. M. Emory. Furthermore, I thank M. D. Sefcik, J. F. Schaefer, and E. O. Stejskal for helpful discussions concerning ^{13}C quantification.

Registry No. Maleic anhydride, 108-31-6; ethylene, 74-85-1.

References and Notes

(1) Carboxyimamidate has also been referred to as N-137 or CARBETHIMER™.
(2) (a) Falk, R. E., et al. *J. Surg. Res.* **1980**, *28*, 485–491. (b) Falk, R. E., et al. *Br. J. Surg.* **1979**, *66*, 861–863. (c) Falk, R. E., et al. *Surgery* **1970**, *84*, 483–489. (d) Fields, J. E.; Asculai, S. S.; Johnson, J. H.; Johnson, R. R. *J. Med. Chem.* **1982**, *25*, 1060–1064.
(3) The structure for hydrolyzed EMA is identical with that of EMA except that the anhydrides have been converted to dicarboxylic acids.
(4) Clerc, J. T.; Pretsch, E.; Sternhell, S. "^{13}C Kernresonzspektroskoper"; Akademische Verlagogesellschaft: Frankfurt am Main, 1973.
(5) (a) Breitmaier, E.; Voelter, W. "^{13}C NMR Spectroscopy"; Verlag Chemie: New York, 1978. (b) Levy, G. C.; Lichter, R. L.; Nelson, G. L. "Carbon-13 Nuclear Magnetic Resonance Spectroscopy"; Wiley: New York, 1980.
(6) The low molecular weight EMA was formed in ethylbenzene whereas the EMA-31 was formed in ethylene dichloride.
(7) The ^1H NMR has a significant absorption, a broad singlet, at approximately 7.8 ppm, which is indicative of an aromatic functionality. The ^{13}C resonances at 144.4 and 128 ppm are consistent with a monoalkylbenzene[6] and under fully relaxed conditions integrate 1:5; the two resonances for maleic acid monomer integrate 1:1 under these same conditions. This eliminates the possibility of hidden vinyl resonances.
(8) The carbonyl resonances (ppm) of benzoic acid and its derivatives are as follows:[5b] acid, 173.5; methyl ester, 167.0; ethyl ester, 164.9.
(9) Of the 10–15 batches of EMA that were examined by ^{13}C NMR, one batch had a very small resonance at 10.2 ppm, which may indicate a small amount of RCH_2CH_3 termination for that particular batch.
(10) The hydrolyzed tetramer was shown to be approximately a 60/40 ratio of *dl*/meso isomers. Ammoniating the tetramer should give the same isomer ratio; therefore resonances 8 and 10 should represent the *dl* form.
(11) The figures referred to are only to illustrate which peaks were being examined and are not necessarily the quantified spectra from which the conclusions were drawn.
(12) 2,3-Pyrazinedicarboxylic acid was an ideal internal standard because it was an easily handled solid whose spectrum did not interfere with those of the copolymers.
(13) The molecular weight of each polymer (p) using this standard (st) can be obtained by using the following equation: $(MW)^p = 2.5(wt)^p \times (integration)^{st}/(moles)^{st}(integration)^p$.
(14) Fields, J. E.; Asculai, S. S.; Johnson, J. H. U.S. Patent 4 255 537, Mar 10, 1981.
(15) The pulse width required for a 90° flip for EMA in water was experimentally found to be 25.2 μs. Therefore 7.7 μs corresponds to a 30° flip.
(16) Formacek, V.; Desnoyer, L.; Kellerhals, H. P.; Clerc, J. T. "^{13}C Data Bank"; Bruker-Physik: Karlsruhe, 1976; Vol. 1.
(17) Breitmaier, E.; Bauer, G. "^{13}C-NMR-Spektroskopie, eine Arbeitsanleitung mit Ubungen"; Georg Theime Verlag: Stuttgart, 1977.

Quasi-Elastic Light Scattering of Poly(hexyl isocyanate) in Hexane†

Kenji Kubota and Ben Chu*

Chemistry Department, State University of New York at Stony Brook, Long Island, New York 11794. *Received February 23, 1982*

ABSTRACT: The field correlation function of light scattered from poly(hexyl isocyanate) (PHIC) in *n*-hexane at 25 °C was analyzed according to the dynamic structure factor of a semiflexible filament as proposed by Fujime, based on the Harris–Hearst model for wormlike chains. In the molecular weight range $M_w > 10^5$, we found the PHIC molecules to be fairly flexible, with $\gamma L = 3.36$ and 6.84 for PHIC with molecular weights of 2.0×10^5 and 4.1×10^5, respectively. In our preliminary analysis, we found excellent agreement between our light scattering results for a non-free-draining polymer (PHIC) in hexane and the free-draining Fujime theory as well as the sedimentation coefficient results of Murakami, Norisuye, and Fujita. Our demonstration suggests that we may have a method that will permit us to determine the flexibility parameter for wormlike polymer chains using Rayleigh line width measurements as a function of the magnitude of the momentum transfer vector, especially when the theory can be modified to include hydrodynamic interactions.

Introduction

Dilute solutions of poly(hexyl isocyanate) (PHIC) were first investigated by Schneider et al.,[1] who showed an unmistakable stiffness of this polymer. Subsequently, Berger and Tidswell[2] and Rubingh and Yu[3] showed that the PHIC chain in tetrahydrofuran and in hexane can be represented by the wormlike chain model. A detailed study has recently been presented by Murakami et al.,[4] who used 19 well-fractionated samples of PHIC ranging in molecular weight from 7×10^4 to 7×10^6 with hexane at 25 °C as a solvent. By means of light scattering, viscosity, and sedimentation velocity measurements, they determined the *z*-average mean square radius of gyration $\langle r_g^2 \rangle_z$, the intrinsic viscosity $[\eta]$, and the sedimentation coefficient s_0 as a function of molecular weight M. A persistence length A (=42 ± 1 nm) and a molar mass per unit contour length M_L (=715 ± 15 nm^{-1}) were computed using the molecular weight dependence of $\langle r_g^2 \rangle_z$ according to the Benoit–Doty theory[5] for the Kratky–Porod wormlike chain. With A and M_L fixed to 42 nm and 715 nm^{-1}, respectively, the data for the intrinsic viscosity $[\eta]$ and the sedimentation coefficient s_0 were then used to compute an

†Work supported by the National Science Foundation, Polymers, Program (Grant DMR 8016521), and the U.S. Army Research Office, Durham, NC.

0024-9297/83/2216-0105$01.50/0

additional hydrodynamic parameter d, the diameter of the cylinder, based on the Yamakawa–Fujii theory.[6,7] It was found that d = 1.6 and 2.5 nm using $[\eta]$ and s_0 data, respectively. Murakami et al.[4] noted that the diameter value (d = 2.5 nm) fitting the s_0 data was seemingly incompatible with the chemical structure of the PHIC repeat unit, estimated to be in a range between 1.2 and 1.8 nm for the helix diameter of poly(butyl isocyanate) from crystallographic data,[8] which agrees with d = 1.6 nm from the intrinsic viscosity data. A similar but reversed discrepancy was encountered in a recent study on DNA by Godfrey and Eisenberg,[9] who found that d = 2.6 nm derived from s_0 data to be in agreement with the diameter of a double-stranded DNA estimated from X-ray diffraction and scattering[10] but in disagreement with d = 1.2 nm derived from intrinsic viscosity data. The discrepancy between the DNA and PHIC experiments and the Yamakawa–Fujii hydrodynamic theory has not yet been resolved. In fact, Hearst and Reese[11] have raised the issue on the values and the significance of the parameters related to the bead diameter and bead spacing of the wormlike coils and pointed out that "Hearst and Stockmayer[12] took the position that the formal validity of continuum hydrodynamics when dealing with molecular dimensions was questionable and therefore the interpretation of the magnitude of parameters, 'such as d', was suspect on fundamental physical grounds". In this article, we have used laser light scattering, including photon correlation spectroscopy, to determine the time correlation function of PHIC as a function of the magnitude of the momentum transfer vector K (=$(4\pi/\lambda)$ sin $(\theta/2)$, with λ and θ being the wavelength of light in the scattering medium and the scattering angle, respectively), concentration, and molecular weight using normal hexane at 25 °C as a solvent. In addition to comparing the translational diffusion coefficient at infinite dilution with s_0, one can analyze the average line width according to the theory of Fujime[13] and co-workers[13-15] for semiflexible filaments in dilute solution.

Experimental Methods

PHIC Sample Preparation. PHIC was synthesized according to the same procedure as reported by Aharoni.[16] Hexyl isocyanate was purchased from Kodak and used without further purification. One gram of NaCN was finely ground and suspended in 50 mL of DMF that had been treated by molecular sieves. The suspension was stirred vigorously for about 1 h before use.

A 300-mL three-neck flask was equipped with a dropping funnel, stirrer, and nitrogen inlet and outlet, which were fitted with Drierite tubes. The three-neck flask containing 20 mL of hexyl isocyanate and 60 mL of DMF was cooled to ca. −79 °C using a dry ice/acetone mixture. With vigorous stirring, 20 mL of the NaCN suspension in DMF was added dropwise through the dropping funnel to the hexyl isocyanate/DMF mixture. After addition of all of the NaCN suspension, 200 mL of 0 °C methanol was added, all at once, with vigorous stirring. The resulting polymer was then filtered, rinsed with methanol, dried, and stored in a desiccator until ready for fractionation.

The fractionation procedure was essentially the same as that reported by Rubingh and Yu[3] with carbon tetrachloride as a solvent and methanol as a precipitant. We extracted eight fractions from which we designated fractions 2, 5, and 7 as samples A, B, and C. n-Hexane was fractionally distilled in the presence of calcium hydride. The fractionated and dried PHIC was weighed and dissolved in purified hexane. A 0.5 wt % stock solution was centrifuged at ~7000g for a few hours. Solutions in the light scattering cells were prepared by diluting known amounts of the middle portion of the centrifuged stock solution with known amounts of filtered (0.22-μm pore size diameter) purified hexane. All cells were flame sealed. The concentration of the middle portion of the centrifuged stock solution was determined by weighing the solution and then the PHIC after evaporation of hexane.

Light Scattering. The light scattering spectrometer has been described in detail elsewhere.[17] We used an argon ion laser operating at λ_0 = 488.0 nm and about 100 mW and a helium neon laser operating at λ_0 = 632.8 nm and about 40 mW. Intensity was measured by means of photon counting and the time correlation function by means of a 96-channel single-clipped correlator. The scattered intensity has been calibrated using benzene and NBS 705 polystyrene in cyclohexane as references, while the Rayleigh line width has been checked using aqueous suspensions of Dow polystyrene latex spheres.

Theoretical Background[14,15]

We shall follow the analysis of Maeda and Fujime to analyze the field correlation function for a semiflexible, wormlike filament in order to see the effect of the filament flexibility on the dynamic light scattering spectrum.

The scattered electric field correlation function has the form

$$g^{(1)}(\tau) = \exp(-DK^2\tau)S(\tau)/S(0) \tag{1}$$

where the dynamic structure factor for internal motion (including the rotational motion of the semiflexible filament) $S(\tau)$ is given by

$$S(\tau) = (1/L^2)\int\int_{-L/2}^{L/2} J(s,s',\tau)\, ds\, ds' \tag{2}$$

and

$$J(s,s',\tau) = \exp[-(K^2/6)\sum_n{}'\langle q_n^2\rangle \times \{Q^2(n,s) + Q^2(n,s') - 2Q(n,s)Q(n,s')\exp(-\tau/\tau_n)\}] \tag{3}$$

The prime on the summation is to denote that n = 0 is excluded and the Q terms have been defined elsewhere.[13] s is the coordinate of a line element ds measured along the chain having length L.

$$\langle q_n^2\rangle = 3D\tau_n L \tag{4}$$

with τ_n being the characteristic decay time of the nth mode.

Kuhn's length, $1/\gamma$, is defined as

$$1/\gamma \equiv 2A \tag{5}$$

and the end-to-end distance $\langle R^2\rangle$ of the Kratky–Porod wormlike chain has the form

$$\langle R^2\rangle = \{\exp(-2\gamma L) - 1 + 2\gamma L\}/2\gamma^2 \tag{6}$$

In the stiff limit ($\gamma L \ll 1$), we retrieve the rigid-rod case:

$$Q(1,s) = (3/L)^{1/2}s/(L/2) \tag{7}$$

while in the flexible limit ($\gamma L \gg 1$), we retrieve the Rouse model:

$$Q(1,s) = (2/L)^{1/2}\sin(\pi s/L) \tag{8}$$

By following the development of Fujime and Maruyama,[14] we obtain

$$g^{(1)}(\tau) = \sum_N\sum_M P_{NM}(Y)\exp\left[-\left(DK^2 + \frac{N}{\tau_1} + \frac{M}{\tau_2}\right)\tau\right] \tag{9}$$

where $P_{NM}(Y)$ is the scattering factor for the NM mode with $Y = K^2L^2/6\gamma L$.

The mean square amplitude $\langle\delta^2\rangle$ of the lateral fluctuations of the shape of the filament has the form[11]

$$\langle\delta^2\rangle = (1/L)\int_{-L/2}^{L/2}\langle\vec{r}(s,t)^2\rangle\, ds = (1/L)\sum_n{}'\langle q_n^2\rangle = \sum_n{}'\langle\delta_n^2\rangle \tag{10}$$

where $\vec{r}$ is the position vector of the element of a macro-

Table I
Molecular Parameters of PHIC in *n*-Hexane at 25 °C

	PHIC-A	PHIC-B	PHIC-C
M_w	5.27×10^4	20.2×10^4	41.1×10^4
$\langle r_g^2\rangle_z^{1/2}$, nm		51.4	79.0
D_0, cm²/s	8.11×10^{-7}	3.17×10^{-7}	1.85×10^{-7}
L,[a] nm	73.7	282	575
γL[b]	0.88	3.36	6.84
k_D, cm³/g	27.3	−263	−242
D_{YF}[c]			
d = 1.6 nm	8.81×10^{-7}	3.30×10^{-7}	1.99×10^{-7}
d = 2.5 nm	7.91×10^{-7}	3.06×10^{-7}	1.88×10^{-7}
D_{RR}[d]			
d = 1.6 nm	7.87×10^{-7}	2.81×10^{-7}	1.57×10^{-7}
d = 2.5 nm	6.89×10^{-7}	2.56×10^{-7}	1.45×10^{-7}
$\langle\delta_1^2\rangle$, cm²		1.89×10^{-11}	4.38×10^{-11}
$\langle\delta_2^2\rangle$ cm²		3.68×10^{-12}	9.95×10^{-12}
$\langle\delta_3^2\rangle$, cm²		1.15×10^{-12}	3.82×10^{-12}
$\langle\delta_4^2\rangle$, cm²		4.42×10^{-13}	1.80×10^{-12}

[a] Calculated from $L = M/M_L$ with $M_L = 715$ nm^{-1}. [b] Calculated from $\gamma = 1/2A$ with $A = 42$ nm. [c] Yamakawa-Fujii theory. [d] Rigid-rod and Broersma's equation.

molecular chain as represented by a continuous, differentiable space curve.

According to eq 4, $\langle\delta_n^2\rangle = L^2(3D\tau_n/L^2)$. We used the measured translational diffusion coefficient $\bar{D}$ and set $D = 3\bar{D}/4$, as has been discussed in ref 13, and computed τ_n according to the expression

$$3D\tau_n/L^2 = 4\gamma L/[(\beta_n L)^4 + (4\gamma L)(L^2/\langle R^2\rangle)(\beta_n L)^2] \quad (n \geq 1) \quad (11)$$

The results for $\langle\delta_n^2\rangle$ are tabulated in Table I.

Results and Discussion

We determined the molecular weight M_w and the radius of gyration $\langle r_g^2\rangle_z^{1/2}$ from Zimm plots using the same approach as described by Murakami et al.[4] The results for PHIC samples A, B, and C are tabulated in Table I. Sample A has a molecular weight of 5.27×10^4 with a small radius of gyration whose magnitude can only be estimated very roughly using an angular distribution of scattered light in the visible range. The molecular weight of PHIC is used to compute the chain length L ($=M_w/M_L$), which is equal to 73.7, 282, and 575 nm for PHIC-A, -B, and -C, respectively. As PHIC polymers are known to have wormlike chains, we need values of the chain length L in order to estimate contributions of internal motions in the system that can be observed at different KL values.

The net photoelectron count single-clipped time correlation functions were fitted to

$$\ln (A\beta)^{1/2}|g^{(1)}(\tau)| = \ln (A\beta)^{1/2} - \bar{\Gamma}\tau + \tfrac{1}{2}(\mu_2/\bar{\Gamma}^2)(\bar{\Gamma}\tau)^2 + B(\bar{\Gamma}\tau)^3 \quad (12)$$

where $\bar{\Gamma}$ is the average decay rate and $\mu_2/\bar{\Gamma}^2$, the normalized dispersion.[18] $\ln (A\beta)^{1/2}$ is an experimentally determined scaling factor. The last term $B(\bar{\Gamma}\tau)^3$, with B being related to the skewness of the line width distribution function, represents the expansion to third order. In our data-analysis procedures, we normally fitted the measured net time correlation function to eq 12 with and without the third-order term in order to check the reliability of $\bar{\Gamma}$ and $\mu_2/\bar{\Gamma}^2$. For samples PHIC-B and PHIC-C with λ_0 = 488 nm and $\theta = 35°$, we have $KL \sim 3$ and 6, which represent second-mode (P_{20}) contributions[15] of about 0.2% and 1%, respectively, as shown in Figure 1.

Rayleigh line width measurements at $\theta = 35°$ using λ_0 = 448.0 nm were further checked at $\theta = 20°$ and 25° using λ_0 = 632.8 nm in a different light scattering spectrometer

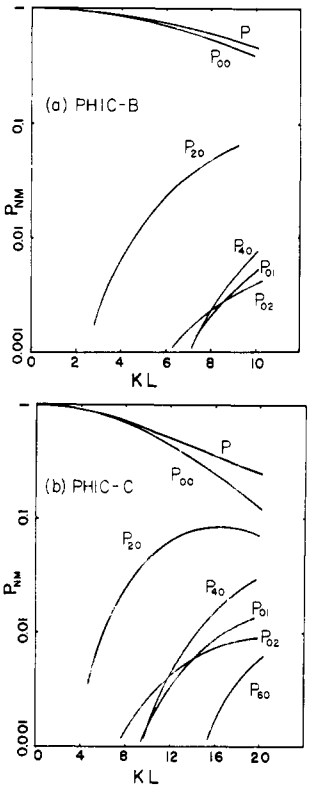

Figure 1. $P_{NM}(Y)$ vs. KL according to the Fujime theory: (a) PHIC-B; (b) PHIC-C. The P_{40} term contributes up to a few percent at $\theta = 135°$, corresponding to $KL \sim 19$ for PHIC-C.

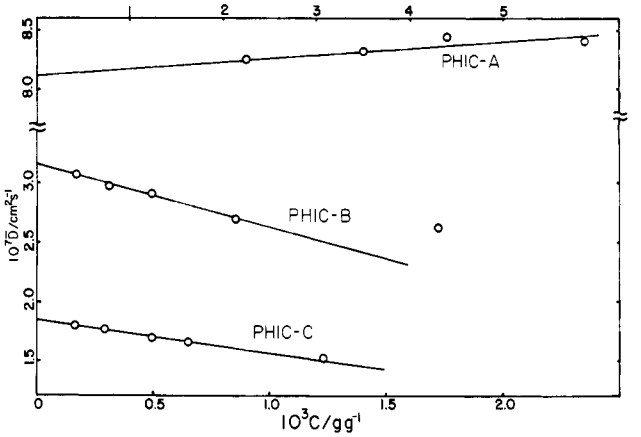

Figure 2. Plots of $\bar{D}$ vs. concentration for PHIC-A, -B and -C in *n*-hexane at 25 °C.

with a similar optical geometry. The low-angle results yield an average line width $\bar{\Gamma}$ and a variance $\mu_2/\bar{\Gamma}^2$, which are related to the translational diffusion coefficient $\bar{D}$ ($=\bar{\Gamma}/K^2$) and the polydispersity of our PHIC samples, respectively. With $\mu_2/\bar{\Gamma}^2 \sim 0.2$–0.3, our fractionated PHIC-A, -B, and -C have molecular weight distributions $M_w/M_n \sim 1.2$–1.3 if we accept the approximate relation $M_w/M_n \approx 1 + \mu_2/\bar{\Gamma}^2$ for rigid-rod polymers. The values are only slightly broader than those reported by Murakami et al.[4] Figure 2 shows the concentration dependence of $\bar{D}$ for PHIC-A, -B, and -C in *n*-hexane at 25 °C. The linear concentration dependence suggests that the PHIC solutions are in the dilute solution region. In particular, for the lower molecular weight sample A, the linear region can be extended to fairly high concentrations while for sample B we have noted a distinct deviation at $C \sim 1.5 \times 10^{-3}$ g/g. The concentration range of our studies is similar to those of Murakami et al.,[4] who have reported a linear concentration

dependence of the osmotic compressibility, in agreement with our findings based on the Zimm plots. According to the Doi–Edwards theory[19] for rod polymer solutions, the overlap concentration C_L^* is defined as

$$C_L^* = M_w/N_A\rho_0 L^3 \quad (13)$$

where N_A and ρ_0 are Avogadro's number and the solvent density, respectively. With M_w and L from Table I, we get $C_L^* = 3.34 \times 10^{-4}$, 2.21×10^{-5}, and 5.30×10^{-6} g/g for PHIC-A, -B, and -C, respectively. The concentration range of our PHIC solutions is between about 1×10^{-4} and 2×10^{-3} g/g, far beyond the overlap concentration C_L^* for rigid-rod polymer solutions. In fact, the linear concentration dependence of the osmotic compressibility, the sedimentation coefficient, and the translational diffusion coefficient in the 1×10^{-4} to 2×10^{-3} g/g concentration range suggests strongly that PHIC solutions of our samples A, B, and C exhibit non-rigid-rod solution behavior. With $A = 42$ nm, we have $\gamma L = 0.877$, 3.36, and 6.84 for PHIC-A, -B, and -C in n-hexane at 25 °C. In the stiff limit, $\gamma L \ll 1$, our PHIC solutions exhibit wormlike behavior, especially for those at higher molecular weights. For coiling macromolecules, the overlap concentration C^* is of the order of $M_w/N_A\rho_0\langle r_g^2\rangle_z^{3/2}$ and is higher than C_L^* by a factor of $(L/\langle r_g^2\rangle_z^{1/2})^3$, corresponding to a factor of 315 and 385 for PHIC-B and -C solutions, respectively. $C^* \sim 7 \times 10^{-3}$ and 2×10^{-3} g/g for PHIC-B and -C solutions, which are greater than the highest concentrations shown in Figure 1. The value of the second virial coefficient A_2 from light scattering intensity measurements[4] remains relatively constant for molecular weights ranging from 5×10^4 to 1.5×10^6. Yet the slopes in plots of $\bar{D}$ vs. concentration, as shown in Figure 2 and Table I, change from positive for PHIC-A to negative for PHIC-B and -C solutions. Therefore the change of sign in the second virial coefficient k_D of the translational diffusion equation

$$\bar{D} = \bar{D}_0 (1 + k_D C) \quad (14)$$

must be related to changes of the hydrodynamic interactions. It should be noted that in the adoption of the Harris–Hearst model[20] by Fujime and Maruyama,[14] hydrodynamic interactions were neglected. We should, therefore, try to justify our comparison of the dynamic line width results for a non-free-draining polymer (PHIC) in hexane with the free-draining theory, especially in very dilute solutions.

The Harris–Hearst model can be extended to polymer solutions in the presence of hydrodynamic interactions. However, the new eigenvalues are not available even though their computation are feasible in principle. In the first approximation, especially for reasonably stiff semiflexible chains (with γL, say, <7), internal motions are less susceptible to changes that are affected by deviations from the free-draining approximation. Therefore, we use the *measured* translational diffusion coefficient in our comparison with the Fujime theory for wormlike chains. At this stage of development, we have noted that the measured values of the translational diffusion coefficient fall within limits of the computed uncertainties based on the Yamakawa–Fujii theory using two different but plausible values of the diameter for PHIC, as shown in Table I. Final quantitative comparison using a modified Harris–Hearst model for non-draining semiflexible chains awaits further theoretical development, including more detailed discussions on the limits of small-scale hydrodynamics related to local internal modes of semiflexible chains.

According to the Yamakawa–Fujii theory[6] (eq 49–52 of ref 6), we can compute the translational diffusion coefficient at infinite dilution using known values of A, M_L, and d. Figure 3 shows log–log plots of $\bar{D}$ vs. molecular weight (M_w) for $M_L = 715$ nm^{-1}, $A = 42$ nm, and $d = 1.6$ nm (solid line) and 2.5 nm (dashed line). The hollow squares denote values of $\bar{D}_0$ computed from s_0 and M_w in Table II of ref 4 using the Svedberg equation:

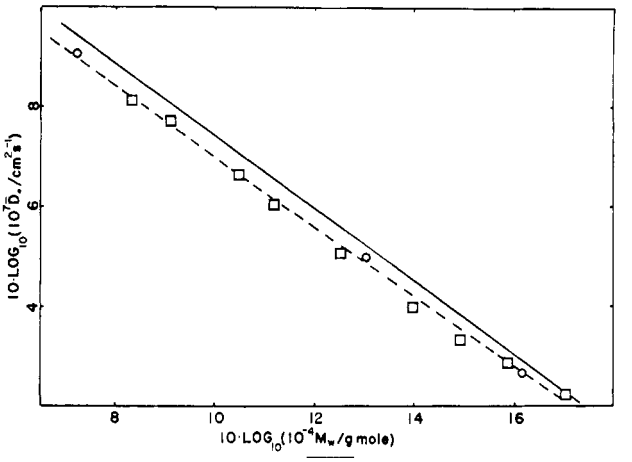

Figure 3. log–log plots of $\bar{D}_0$ vs. M_w for PHIC in n-hexane at 25 °C. Hollow circles denote measured $\bar{D}_0$ by extrapolation to infinite dilution using photon correlation spectroscopy. Hollow squares denote $\bar{D}_0$ values computed from measured s_0 in Table II of ref 4. The solid and dashed curves are based on the Yamakawa–Fujii theory using $M_L = 715$ nm^{-1}, $A = 42$ nm, and $d = 1.6$ nm and 2.5 nm, respectively.

$$s_0 = \frac{M_w(1 - \bar{v}\rho_0)}{N_A k_B T} D_0 \quad (15)$$

where we have taken the density of n-hexane to be 0.655 g/cm^3 and the partial specific volume ($\bar{v}$) of PHIC in n-hexane at 25 °C to be 0.950 cm^3/g. The hollow circles are the $\bar{D}_0$ values from Figure 2. Our light scattering measurements are in very good agreement with the sedimentation coefficient results of Murakami et al.[4] The value of the diameter $d = 2.5$ nm is in disagreement with the diameter computed from intrinsic viscosity data and the chemical structure of the PHIC repeat unit from crystallographic data, estimated to be about 1.6 nm. The discrepancy in the diameter of the molecular chain from the diffusion coefficient/sedimentation coefficient and from the X-ray crystallographic data is perhaps not unreasonable as the X-ray results yield a static value while the diffusion coefficient and the sedimentation coefficient experiments deal with an effective hydrodynamic diameter using a theory that has not taken into account the lateral vibration of wormlike chains. However, we then have difficulty in explaining why the intrinsic viscosity results agree with the X-ray crystallographic data.

In order to demonstrate the flexibility of PHIC-B and -C polymers in n-hexane, we have plotted $Q(1,s)L^{1/2}$ as a function of $s/(L/2)$ as shown in Figure 4, using $\gamma L = 3.36$ and 6.84 for PHIC-B and -C, respectively. Figure 4 shows that with $\gamma L \sim 7$ PHIC-C behaves much more like a polymer coil in the Rouse limit than a wormlike chain. Even at $M_w \sim 2 \times 10^5$ for PHIC-B, the polymer chain is far from stiff.

According to eq 9, the time correlation $g^{(1)}(\tau)$ can be computed using known values of M_L and A. Here, we have taken D as the measured translational diffusion coefficient at a finite concentration C. The number of time-dependent terms (τ_1, τ_2, ...) is limited to τ_2 because the nth normal mode (τ_n) will contribute to the correlation function only if $\langle\delta_n^2\rangle > 1/K^2$. At $\theta = 35°$ and 135°, $1/K^2 = 8.80 \times 10^{-11}$ and 9.32×10^{-12} cm^2, respectively. With $\langle\delta_n^2\rangle$ values listed in Table I, modes up to the τ_2 term should

Table II
Specific Numerical Results Based on Eq 6-9 and 27 for PHIC-B and PHIC-C in *n*-Hexane at 25 °C

	PHIC-B				PHIC-C			
n	$\alpha_n L/2$	$\beta_n L/2$	C_n	$3D\tau_n/L^2$	$\alpha_n L/2$	$\beta_n L/2$	C_n	$3D\tau_n/L^2$
1	3.947	1.514	1.822	2.354×10^{-2}	7.277	1.561	1.965	1.326×10^{-2}
2	4.660	2.904	1.659	4.590×10^{-3}	7.746	3.079	1.900	3.008×10^{-3}
3	5.633	4.295	1.524	1.436×10^{-3}	8.443	4.556	1.833	1.156×10^{-3}
4	6.801	5.741	1.400	5.515×10^{-4}	9.314	6.020	1.757	5.442×10^{-4}
5	8.101	7.235	1.305	2.447×10^{-4}	10.325	7.489	1.670	2.861×10^{-4}
6	9.486	8.758	1.240	1.218×10^{-4}	11.449	8.976	1.582	1.620×10^{-4}
7	10.924	10.298	1.197	6.643×10^{-5}	12.663	10.480	1.502	9.714×10^{-5}
8	12.396	11.849	1.168	3.897×10^{-5}	16.663	15.071	1.335	2.712×10^{-5}

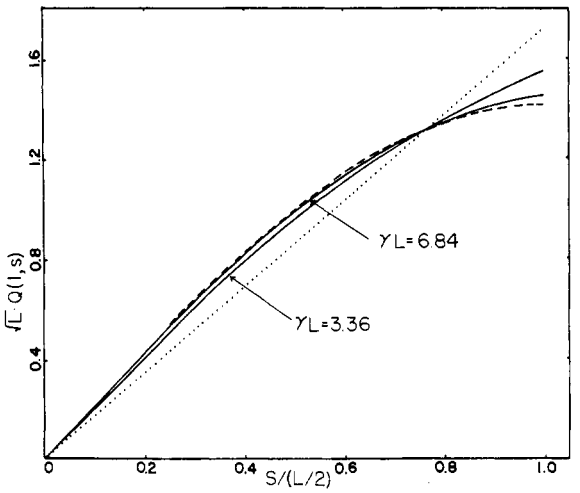

Figure 4. Plots of $Q(1,s)L^{1/2}$ vs. $s/(L/2)$: dashed line, flexible limit ($\gamma L \gg 1$), eq 8; dotted line, stiff limit ($\gamma L \ll 1$), eq 7; PHIC-B ($\gamma L = 3.36$), Fujime theory; PHIC-C ($\gamma L = 6.84$), Fujime theory.

be sufficient for computing $|g^{(1)}(\tau)|$. The actual $\beta_n L/2$ and $\alpha_n L/2$ values used in computing $|g^{(1)}(\tau)|$ are listed in Table II for PHIC-B and -C in *n*-hexane. The $3D\tau_n/L^2$ values are computed according to eq 11 and τ_n is then calculated using known values of $\bar{D}$ and L. The computed $|g^{(1)}(\tau)|$ values are then fitted to eq 12 to obtain $\bar{\Gamma}$ for the Harris–Hearst model of wormlike chains. In the flexible limit at infinite dilution[20]

$$|g^{(1)}(\tau)| = S(K,t)/S(K,0) \tag{16}$$

where

$$S(K,t) = S_0(X)\exp(-D_0K^2t) + S_2(X^2)\exp(-(K^2D_0 + 2/\tau_1)t) + \ldots \tag{17}$$

and

$$S_0(X^2) = (\pi/X)\exp(-X/6)(\mathrm{erf}\,(X^{1/2}/2))^2 \tag{18}$$

with

$$\mathrm{erf}\,(y) \equiv 1/\pi^{1/2}\int_0^y \exp(-Z^2)\,dZ$$

$$X \equiv K^2 r_g^2$$

and

$$\tau_1 = 2r_g^2/\pi^2 D_0$$

The results based on the Harris–Hearst model (solid curve) and the Rouse model (dashed curve) as well as the limiting $\bar{\Gamma}$ ($\equiv \bar{D}K^2$) value due to pure translational motion of the polymer chain (solid line) are compared with the measured $\bar{\Gamma}$ values (hollow circles) in Figure 5 for PHIC-B (Figure 5a) and PHIC-C (Figure 5b). The agreement between our measured $\bar{\Gamma}$ values and those computed according to the Harris–Hearst model (eq 17) is remarkable!

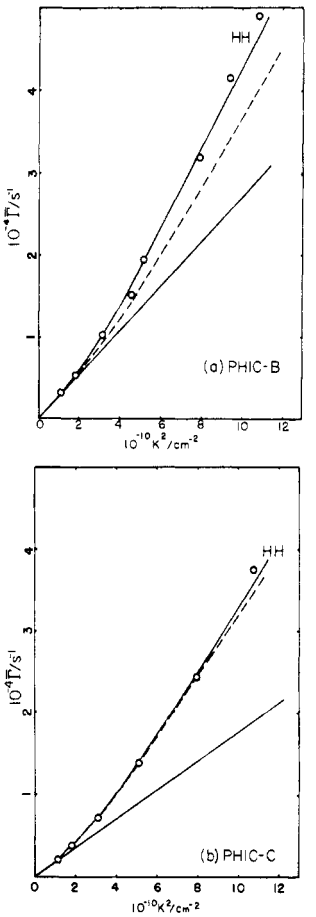

Figure 5. Plots of $\bar{\Gamma}$ vs. K^2. HH denotes computed $\bar{\Gamma}$ based on eq 9. Dashed line denotes the Rouse model (eq 16–18 up to the τ_1 term). Solid line denotes the limiting pure translational motion. Hollow circles denote measured average line width using the method of cumulants up to third order. (a) PHIC-B in *n*-hexane at 25 °C with $\bar{D} = 2.69 \times 10^{-7}$ cm^2/s at $C = 8.49 \times 10^{-4}$ g/g. (b) PHIC-C in *n*-hexane at 25 °C with $\bar{D} = 1.77 \times 10^{-7}$ cm^2/s at $C = 2.88 \times 10^{-4}$ g/g.

In computing the Harris–Hearst curve in Figure 5, the parameters M_L and A came from independent static measurements such as the radius of gyration and the molecular weight and were independent of our dynamic measurements. There are no adjustable parameters for computing the internal motions. We have demonstrated that the semiflexible filament approach of Fujime and co-workers based on the Harris–Hearst model represents an excellent first approximation to visualize the dynamical properties of wormlike chains. More importantly, we can estimate the flexibility parameter ($\gamma L \lesssim 7$) by using the deviations of the K^2 dependence in a $\bar{\Gamma}$ vs. K^2 plot as shown in Figure 5. In this approach we do not need a series of different molecular weight samples as in the case of static measurements. This simplification is especially important in the characterization of biological macromolecules, where

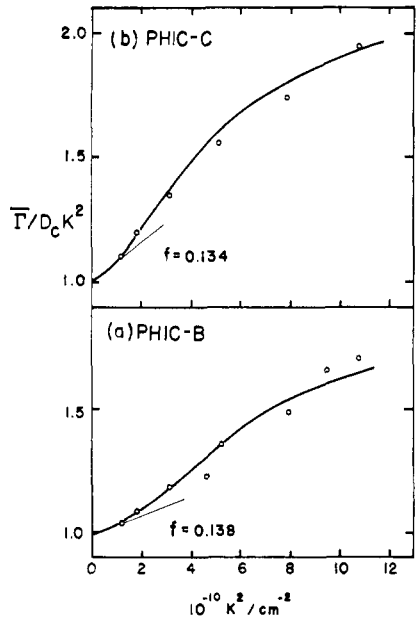

Figure 6. Plots of $\bar{\Gamma}/D_C K^2$ vs. K^2. Same conditions as in Figure 5.

it is often extremely difficult to prepare a series of samples with different molecular weights.

The agreement of the measured (D_0) and the calculated (D_{YF}) values for the non-free-draining translational diffusion coefficient as shown in Table I and the concentration dependence of $\bar{D}$ as shown in Figure 2 indicate that PHIC in *n*-hexane represents a non-free-draining polymer in solution whose hydrodynamic interactions cannot be neglected. Accordingly, our use of a free-draining theory to evaluate the characteristic times of internal modes of a non-free-draining polymer is susceptible to criticism and can, at best, be considered as a first approximation where we have taken the hydrodynamic interactions on internal modes of a relatively stiff ($\gamma L < 7$) semiflexible chain to be a second-order effect.

In the free-draining limit, the angular dependence of $\bar{\Gamma}/q^2$ has been shown to contain information on the structure of the chain stiffness[21] as

$$\bar{\Gamma}/D_C K^2 = 1 + fu^2 + \ldots \qquad (19)$$

where $u^2 = K^2 \langle r_g^2 \rangle_z$ and f is the initial slope corresponding to $^1/_3$, 0.1733, and 0.1 for Rouse chains, Zimm chains, and infinitely thin rigid rods, respectively. We have taken D_C to be the translational diffusion coefficient at concentration C. The values of D_C in Figure 6 was determined by extrapolating $\bar{\Gamma}/K^2$ at concentration C to $K = 0$ in a plot of $\bar{\Gamma}/K^2$ vs. K^2. In dilute solution, $\bar{D} \to D_0$ as $C \to 0$. At $C = 8.49 \times 10^{-4}$ g/g, a nonnegligible difference between D_C and D_0 is involved for PHIC-B while at $C = 2.88 \times 10^{-4}$ g/g for PHIC-C, D_C is much closer to D_0. We present Figure 5 as the unmanipulated average line width data for PHIC-B and PHIC-C at two finite concentrations. By replotting the data of Figure 5 as shown in Figure 6, we are able to estimate f to be 0.13 and 0.14 for PHIC-B ($\gamma L = 3.36$) and PHIC-C ($\gamma L = 6.84$), respectively. In another recent study, we also obtained $f \sim 0.11$–0.12 for the stiffer PBLG molecules. Our estimates of f are precise to within ±15% and depend upon the values of D_C. With $\gamma L \sim 3$–7, f (=0.13–0.14) falls below recent theoretical estimates of Stockmayer and Schmidt,[22] including discussions on preaveraging and nonpreaveraging of the Ossen tensor.

In Figure 6, we have assumed the chain stiffness to be relatively independent of concentration in the dilute solution region. In addition, in our determination of $\bar{\Gamma}$, we did set $\bar{\Gamma}\tau_{max} \sim 3$ as a criterion of our line width measurements, where τ_{max} is the maximum delay time range. With an equally spaced 92-channel correlator, the delay time per channel $\Delta\tau$ (=(3/92)$\bar{\Gamma}$) sets an upper measurable frequency limit corresponding to $1/2\Delta\tau$ according to the Shannon information theory. Therefore, the experimental $\bar{\Gamma}$ values represent a low limit since some high-frequency components may possibly be missed in our measurements. The S-shape curve in Figure 6 resembles the Rouse–Zimm model. The stiffness of PHIC tends to suppress the deviation from the K^2 dependence.

The final conclusion awaits further developments in the theoretical framework where preaveraging and nonpreaveraging of the Ossen tensor are yielding different results and perhaps bending motions need to be included. The physical meaning for a maximum in f for wormlike chains near $\gamma L \sim 10$ in an f vs. γL plot is not clear.

Our preliminary results on PHIC in *n*-hexane confirms the wormlike chain behavior of such polymers with $M \gtrsim 10^4$. For $\gamma L \sim 7$, Figure 5b suggests that the flexibility has reached near the Rouse chain limit experimentally. Therefore, a determination of the flexibility parameter for wormlike polymer chains is limited to $\gamma L \lesssim 7$ even if we are able to modify the Harris–Hearst model to include hydrodynamic interactions. Nevertheless, the present work serves as a first experimental step pointing toward the possibility of determining the flexibility parameter of relatively stiff semiflexible polymer chains ($\gamma L \leq 7$) by observing the angular dependence of the average line width. More detailed studies including other polymer systems are in progress.

Registry No. PHIC, 26746-07-6; poly[(hexylimino)carbonyl], 37727-37-0.

References and Notes

(1) Schneider, N. S.; Furusaki, S.; Lenz, R. W. *J. Polym. Sci., Part A* **1965**, *3*, 933.
(2) Berger, M. N.; Tidswell, B. M. *J. Polym. Sci., Part C* **1973**, *42*, 1063.
(3) Rubingh, D. N.; Yu, H. *Macromolecules* **1976**, *9*, 681.
(4) Murakami, H.; Norisuye, T.; Fujita, H. *Macromolecules* **1980**, *13*, 345.
(5) Benoit, H.; Doty, P. *J. Phys. Chem.* **1953**, *57*, 958.
(6) Yamakawa, H.; Fujii, M. *Macromolecules* **1973**, *6*, 407.
(7) Yamakawa, H.; Fujii, M. *Macromolecules* **1974**, *7*, 128.
(8) Shmueli, U.; Traub, W.; Rosenbeck, K. *J. Polym. Sci., Part A-2* **1969**, *7*, 515.
(9) Godfrey, J. E.; Eisenberg, H. *Biophys. Chem.* **1976**, *5*, 301.
(10) Bloomfield, V. A.; Crothers, D. M.; Tinoco, I. "Physical Chemistry of Nucleic Acids"; Harper and Row: New York, 1974; Chapter 5.
(11) Hearst, J. E.; Reese, D. A. *J. Chem. Phys.* **1980**, *73*, 3007.
(12) Hearst, J. E.; Stockmayer, W. H. *J. Chem. Phys.* **1962**, *37*, 1425.
(13) Fujime, S. *J. Phys. Soc. Jpn.* **1970**, *29*, 751; **1971**, *31*, 1805.
(14) Fujime, S.; Maruyama, M. *Macromolecules* **1973**, *6*, 237.
(15) Maeda, T.; Fujime, S. *Macromolecules* **1981**, *14*, 809.
(16) Aharoni, S. M. *Macromolecules* **1979**, *12*, 94.
(17) DiNapoli, A. Ph.D. Thesis, State University of New York, 1980.
(18) Koppel, D. E. *J. Chem. Phys.* **1972**, *57*, 4814.
(19) Doi, M.; Edwards, S. F. *J. Chem. Soc., Faraday Trans. 2* **1978**, *74*, 560.
(20) Harris, R. A.; Hearst, J. E. *J. Chem. Phys.* **1966**, *44*, 2595.
(21) Burchard, W.; Schmidt, M.; Stockmayer, W. H. *Macromolecules* **1980**, *13*, 1265.
(22) Stockmayer, W. H.; Schmidt, M. *Pure Appl. Chem.* **1982**, *54*, 407.